

Supporting information for

**Synthesis and Structures of Diaryloxystannylenes and -plumbylenes
embedded in 1,3-Diethers of Thiacalix[4]arene**

Ryunosuke Kuriki, Takuya Kuwabara,* and Youichi Ishii*

Department of Applied Chemistry, Faculty of Science and Engineering, Chuo University, 1-13-27, Kasuga, Bunkyo-ku, Tokyo 112-8551,
Japan

Table of contents

1. Details for the X-ray diffraction analysis	S1
2. Molecular structures of thiacalix ^{t-Bu} (OH) ₂ (OSi ⁱ Pr ₃) ₂ (4)	S2
3. X-ray crystallographic data for 2-Sn , 2-Pb , 4 , 5-Sn , and 5-Pb	S3
4. ¹ H, ¹³ C{ ¹ H}, ²⁹ Si{ ¹ H}, ¹¹⁹ Sn{ ¹ H} and ²⁰⁷ Pb NMR spectra of the products	S4–12
5. References	S13

1. Details for the X-ray diffraction analysis

Diffraction data for **2-Sn**, **2-Pb**, **4**, **5-Sn**, and **5-Pb** were collected on a VariMax Saturn CCD diffractometer with graphite-monochromated Mo K α radiation ($\lambda = 0.71075 \text{ \AA}$) at $-180 \text{ }^{\circ}\text{C}$. Intensity data were corrected for Lorentz-polarization effects and for empirical absorption (REQAB).¹ All calculations were performed using the CrystalStructure² crystallographic software package except for refinements, which were performed using SHELXL-2018/3.³ All non-hydrogen atoms were refined on F_o^2 anisotropically by full-matrix least-square techniques. All hydrogen atoms were placed at the calculated positions with fixed isotropic parameters.

2. Molecular structures of thiacalix^{t-Bu}(OH)₂(OSiⁱPr₃)₂ (**4**).

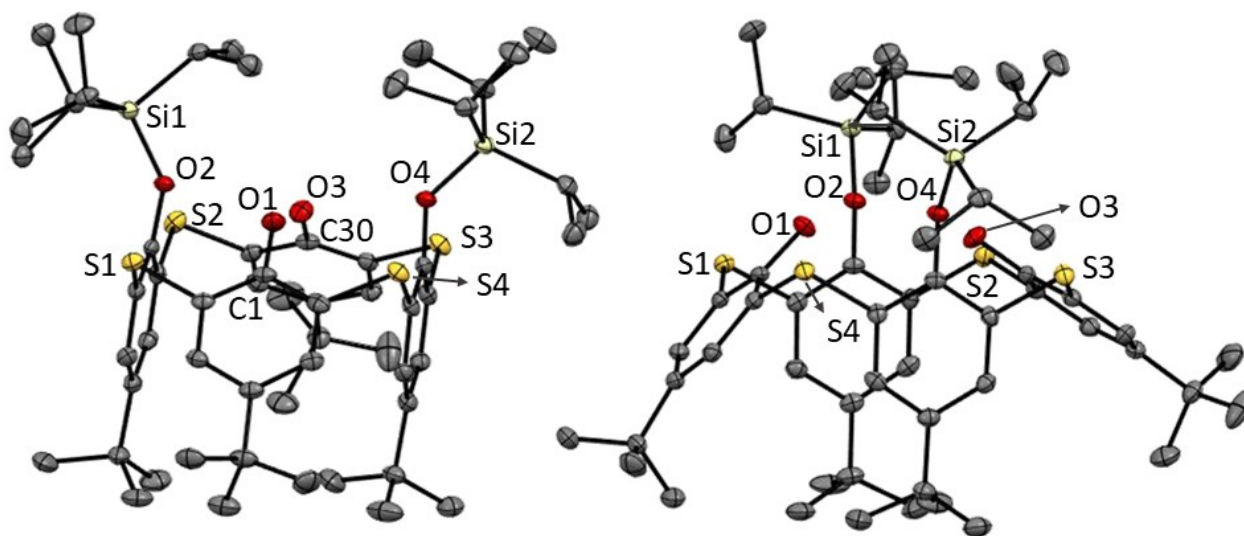


Figure S1. Molecular structures of **4** with thermal ellipsoid plots at 30 % probability. All hydrogen atoms and a THF molecule are omitted for clarity. Selected bond lengths [Å]: C1–O1 1.359(3); C30–O2 1.358(3).

3. X-ray crystallographic data for 2-Sn, 2-Pb, 4, 5-Sn, and 5-Pb.

Table S1. X-ray crystallographic data.

	2-Sn·(Tol) ₃	2-Pb·(Tol)	4·(THF)	5-Sn	6-Pb·(C ₅ H ₁₂) ₂
CCDC	2016537	2021967	2021969	2016539	2021968
formula	C ₇₅ H ₈₂ O ₄ S ₄ Sn	C ₆₁ H ₆₆ O ₄ PbS ₄	C ₆₂ H ₉₆ O ₅ S ₄ Si ₂	C ₅₈ H ₈₆ O ₄ S ₄ Si ₂ Sn	C ₁₃₁ H ₂₀₈ O ₈ Pb ₂ S ₈ Si ₄
fw	1294.33	1198.56	1105.8	1150.37	2694.18
crystal dimension	0.17 × 0.15 × 0.05	0.14 × 0.14 × 0.09	0.16 × 0.14 × 0.06	0.18 × 0.17 × 0.10	0.18 × 0.17 × 0.15
crystal system	triclinic	monoclinic	triclinic	monoclinic	triclinic
space group	<i>P</i> -1	<i>C</i> 2/ <i>c</i>	<i>P</i> -1	<i>P</i> 2 ₁ / <i>c</i>	<i>P</i> -1
<i>a</i> [Å]	12.094(3)	22.413(3)	13.510(2)	13.3770(12)	13.4391(8)
<i>b</i> [Å]	12.497(3)	20.959(2)	15.106(2)	17.7497(15)	13.7334(7)
<i>c</i> [Å]	22.902(6)	12.5139(14)	16.040(2)	25.887(2)	20.3149(10)
α [deg]	83.617(10)	90	79.593(5)	90	71.319(3)
β [deg]	85.056(11)	108.6460(10)	81.074(4)	102.696(2)	77.604(3)
γ [deg]	75.959(9)	90	89.230(6)	90	77.966(3)
<i>V</i> [Å ³]	3330.9(15)	5570.1(11)	3180.1(8)	5996.3(9)	3429.3(3)
<i>Z</i>	2	4	2	4	1
ρ_{calcd} [g cm ⁻³]	1.29	1.429	1.155	1.274	1.305
<i>F</i> (000)	1356	2440	1200	2432	1406
μ [cm ⁻¹]	5.57	32.24	2.32	6.48	26.59
transmission					
factors	0.8455 – 1	0.8697 – 1	0.8616 – 1	0.8793 – 1	0.8718 – 1
range					
index range	-15 ≤ <i>h</i> ≤ 13	-28 ≤ <i>h</i> ≤ 22	-17 ≤ <i>h</i> ≤ 17	-17 ≤ <i>h</i> ≤ 17	-11 ≤ <i>h</i> ≤ 16
	-16 ≤ <i>k</i> ≤ 15	-27 ≤ <i>k</i> ≤ 26	-16 ≤ <i>k</i> ≤ 19	-22 ≤ <i>k</i> ≤ 23	-16 ≤ <i>k</i> ≤ 16
	-29 ≤ <i>l</i> ≤ 29	-16 ≤ <i>l</i> ≤ 16	-15 ≤ <i>l</i> ≤ 20	-33 ≤ <i>l</i> ≤ 29	-25 ≤ <i>l</i> ≤ 25
no. reflections	26547	22455	26240	48104	25173
unique (<i>R</i> _{int})	14566 (0.0636)	6294 (0.0366)	14039 (0.0411)	13722 (0.0396)	13148 (0.0316)
<i>I</i> > 2σ(<i>I</i>)	11317	5736	10139	11958	11126
no. parameters	795	338	684	646	742
<i>R</i> ₁ (<i>I</i> > 2σ(<i>I</i>)) ^a	0.0851	0.0319	0.0598	0.0372	0.0271
<i>wR</i> ₂ (all data) ^b	0.1827	0.0695	0.1488	0.0899	0.0683
GOF ^c	1.098	1.117	1.083	1.118	1.06
max diff peak / hole [e Å ⁻³]	1.297/-1.222	1.5/-1.746	0.475/-0.454	0.48/-0.989	1.635/-1.413

^a $R_1 = \sum ||F_o| - |F_c|| / \sum |F_o|$. ^b $wR_2 = [\sum \{w(F_o^2 - F_c^2)^2\} / \sum w(F_o^2)^2]^{1/2}$, $w = 1/[\sigma^2 F_o^2 + (aP)^2 + bP]$ (*a* and *b* are constants suggested by the refinement program; $P = [\max(F_o^2, 0) + 2F_c^2]/3$). ^c GOF = $[\sum w(F_o^2 - F_c^2)^2 / (N_{\text{obs}} - N_{\text{params}})]^{1/2}$.

4. ^1H and $^{13}\text{C}\{^1\text{H}\}$ NMR spectra of the products

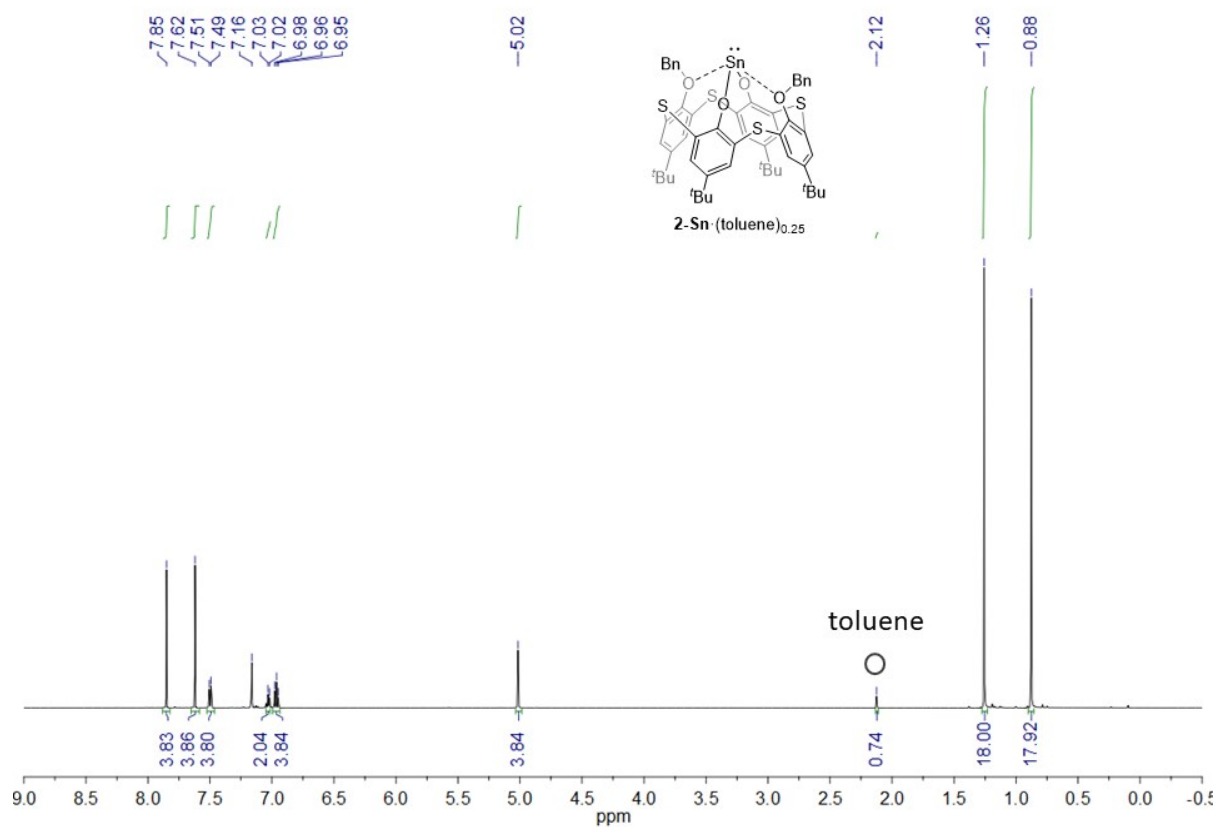


Figure S2. ^1H NMR spectrum of $2\text{-Sn}\cdot(\text{toluene})_{0.25}$ recorded at 50 °C.

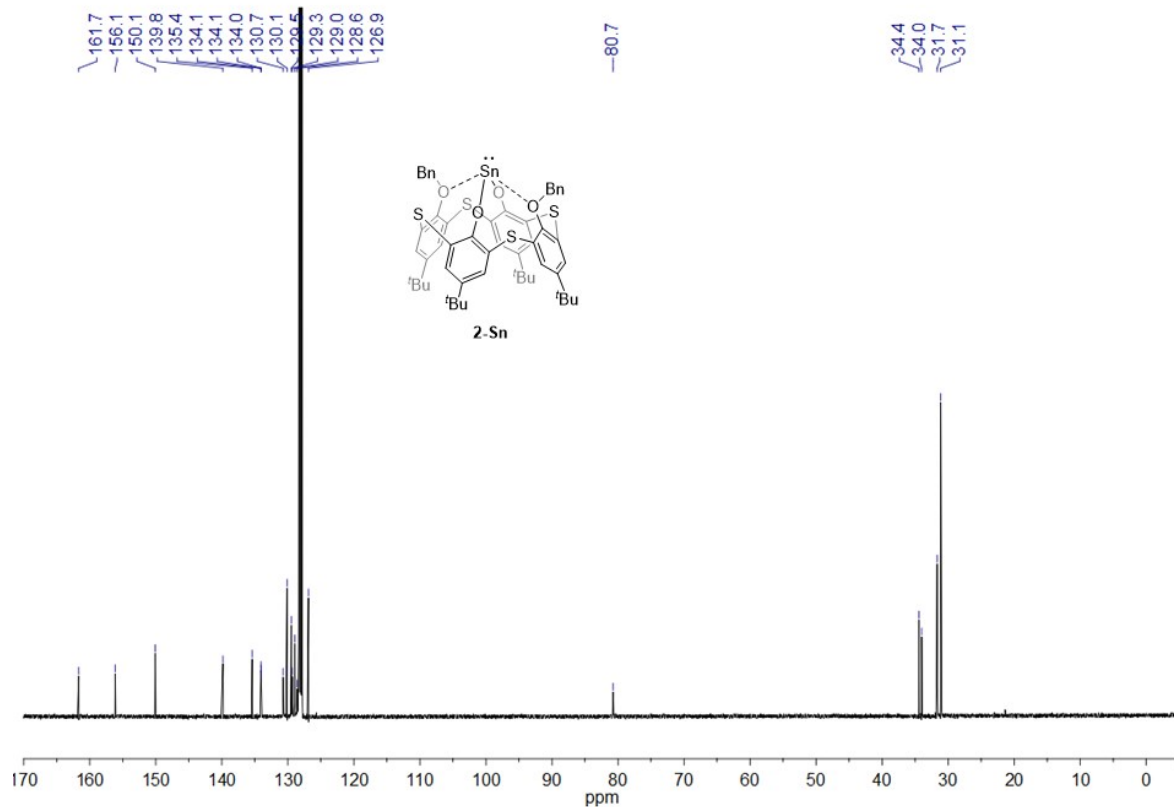


Figure S3. $^{13}\text{C}\{^1\text{H}\}$ NMR spectrum of 2-Sn recorded at 50 °C.

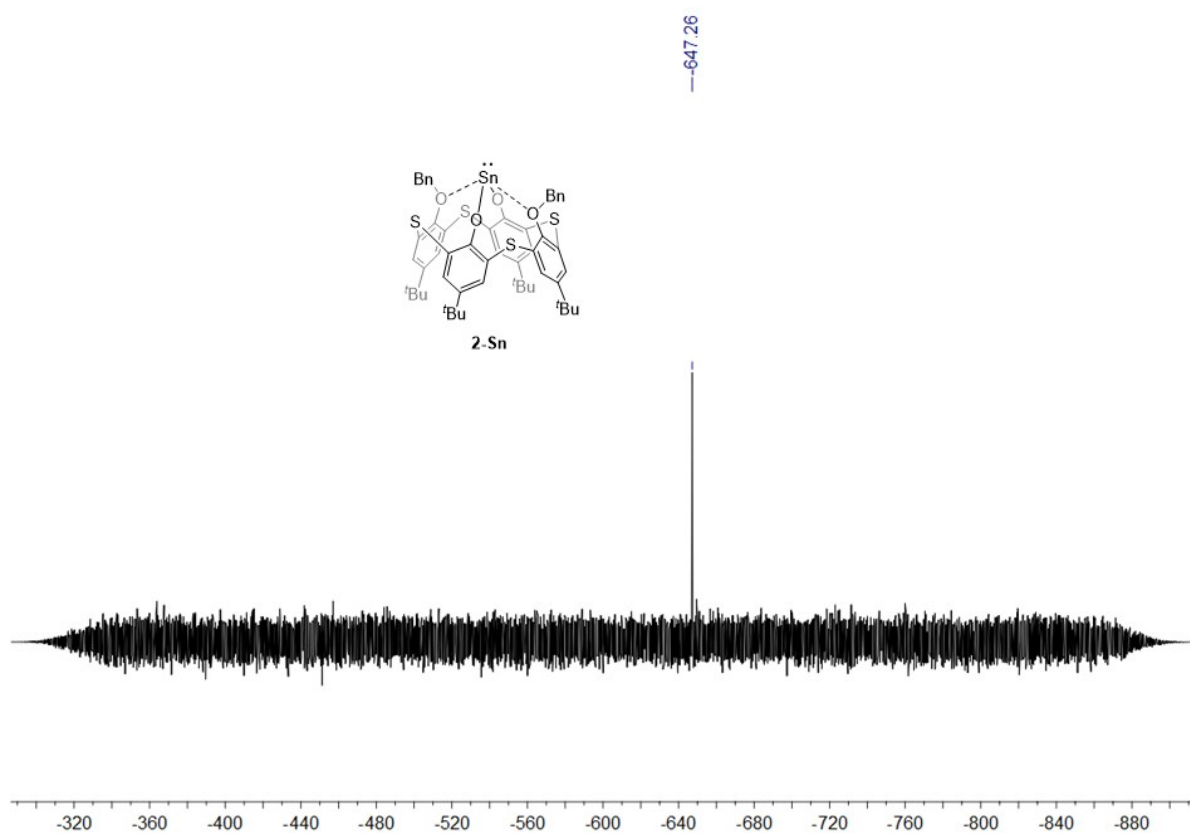


Figure S4. $^{119}\text{Sn}\{^1\text{H}\}$ NMR spectrum of **2-Sn** recorded at 50 °C.

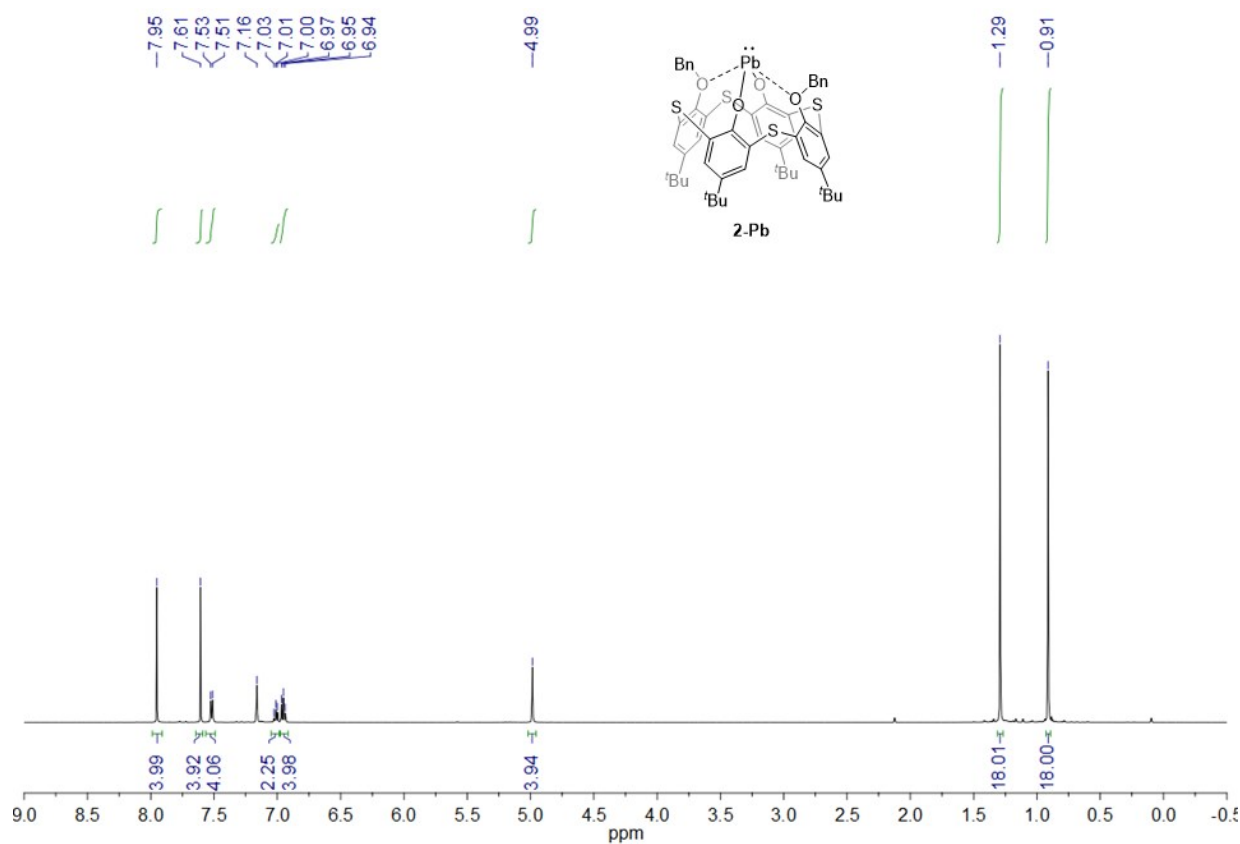


Figure S5. ^1H NMR spectrum of **2-Pb** recorded at 50 °C.

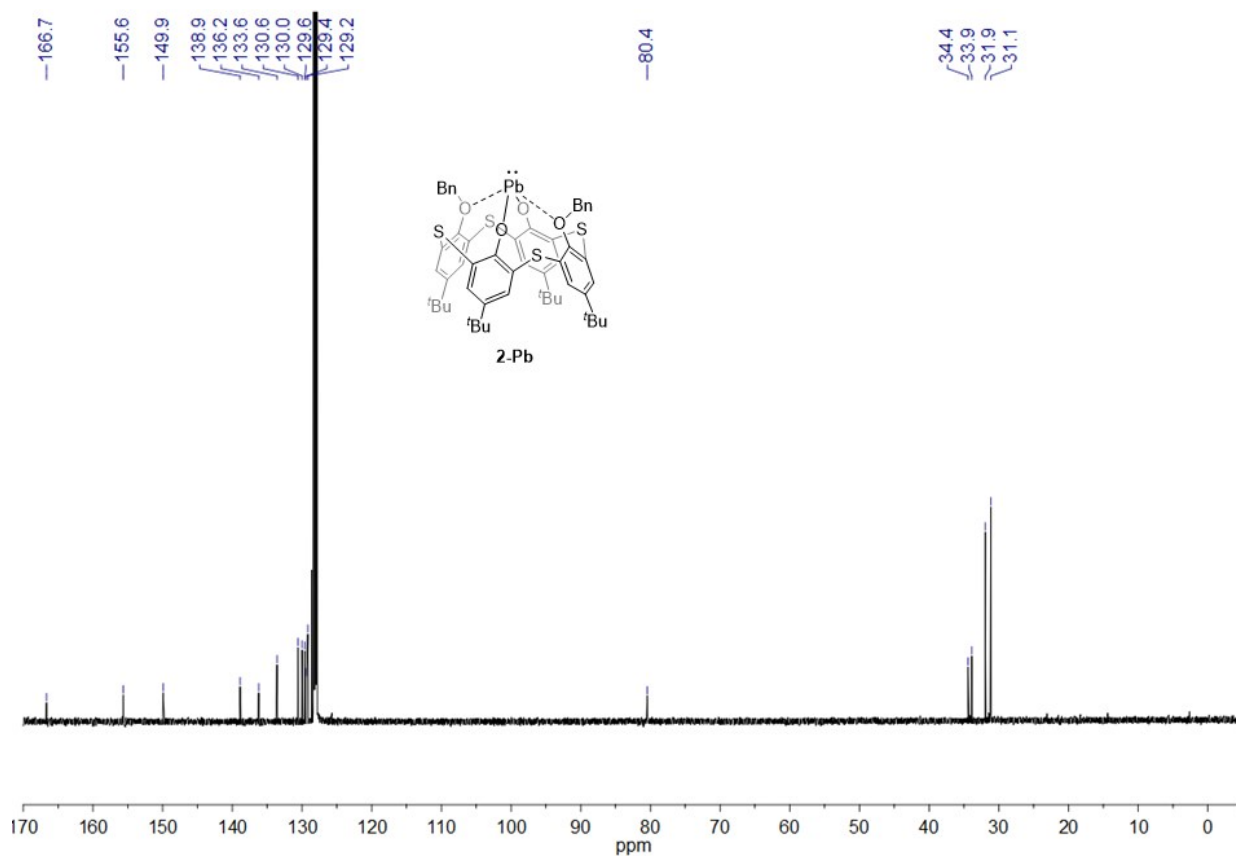


Figure S6. $^{13}\text{C}\{^1\text{H}\}$ NMR spectrum of **2-Pb** recorded at 50 °C.

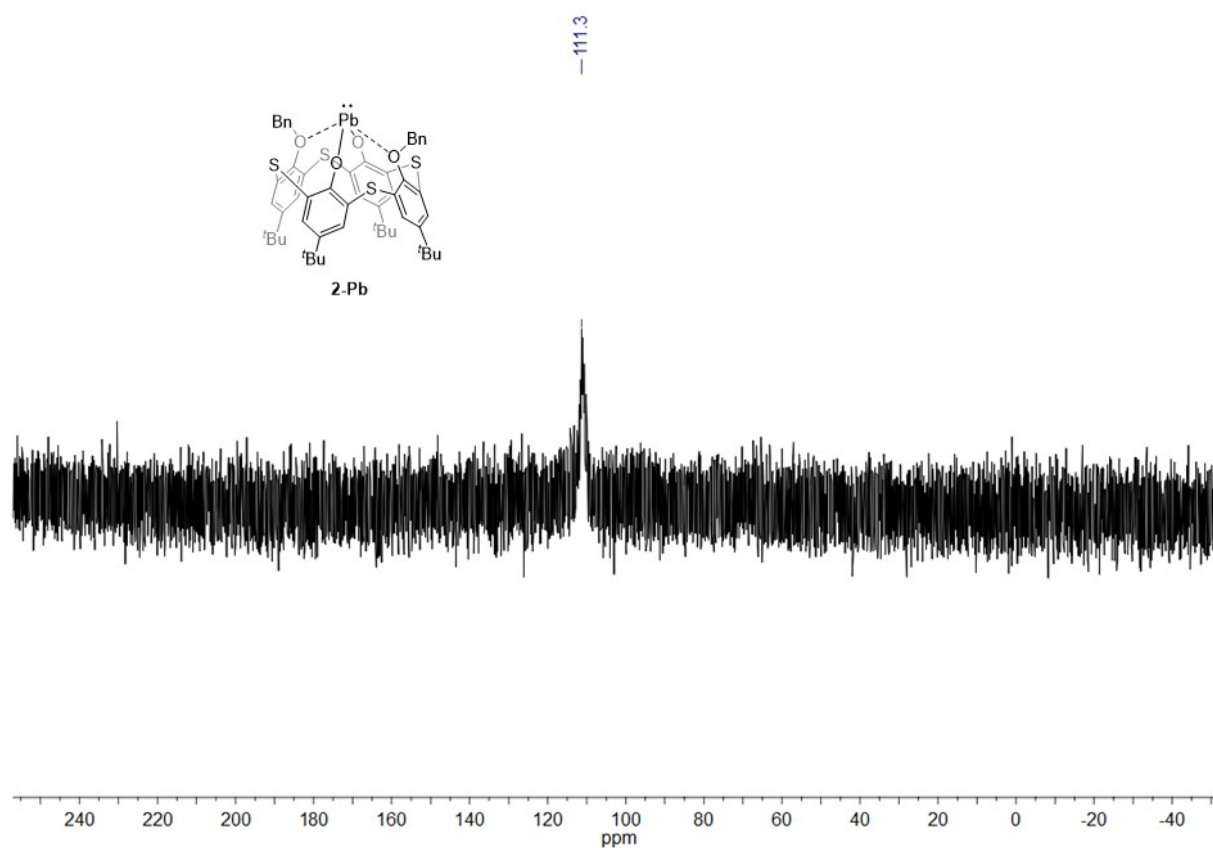


Figure S7. ^{207}Pb NMR spectrum of **2-Pb** recorded at 50 °C.

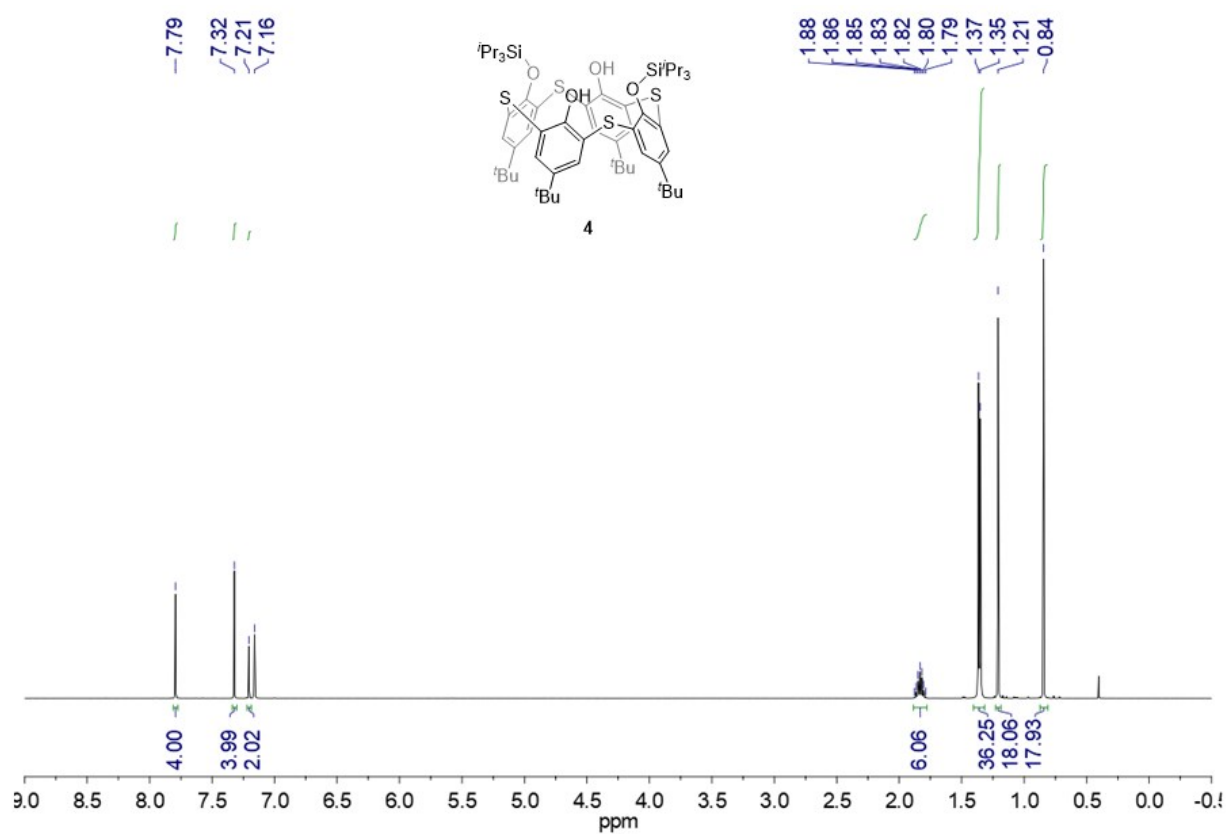


Figure S8. ¹H NMR spectrum of **4**.

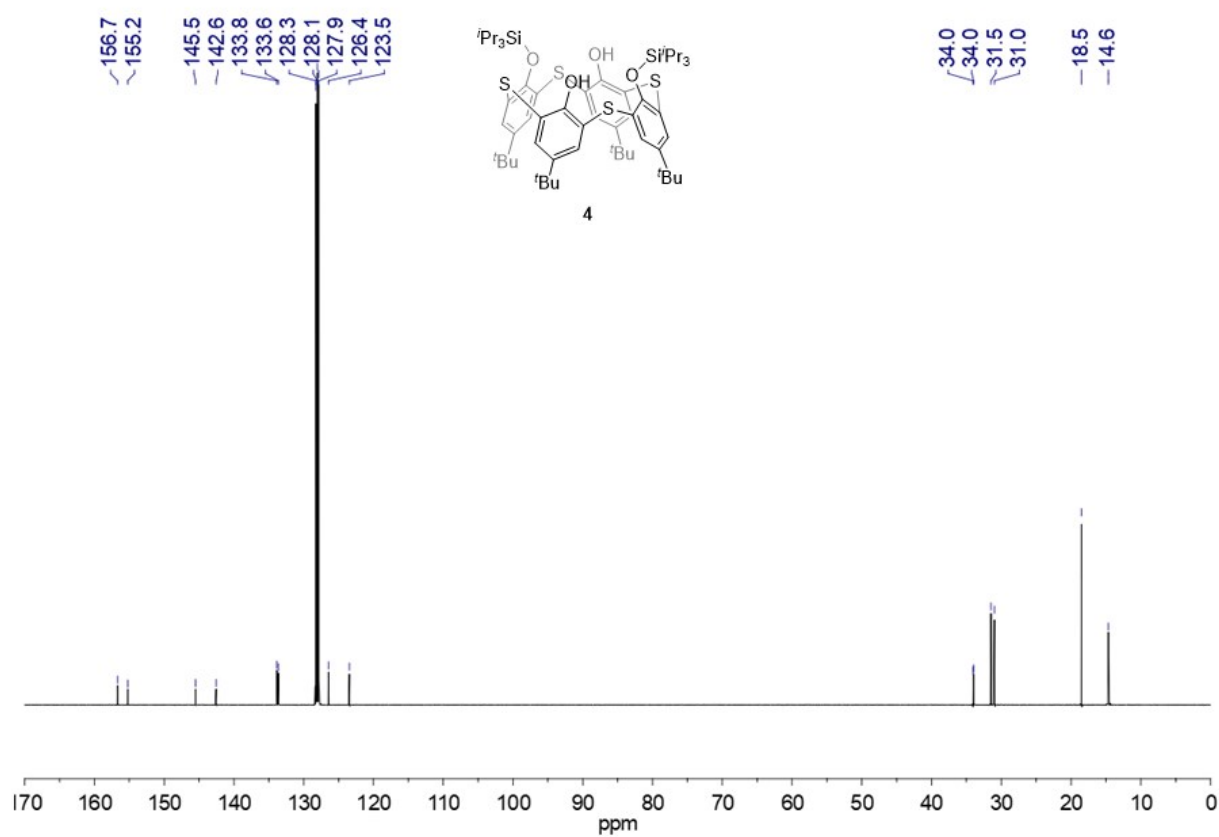


Figure S9. ¹³C{¹H} NMR spectrum of **4**.

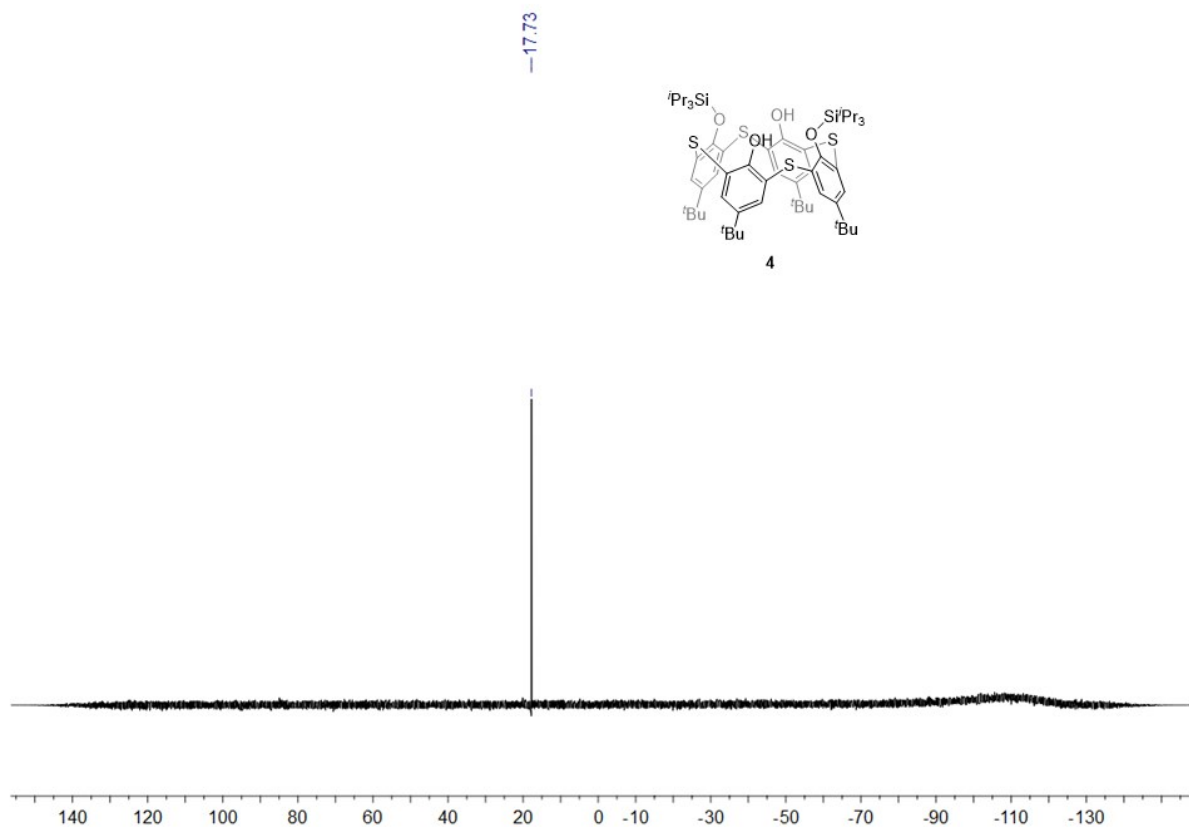


Figure S10. $^{29}\text{Si}\{^1\text{H}\}$ NMR spectrum of **4**.

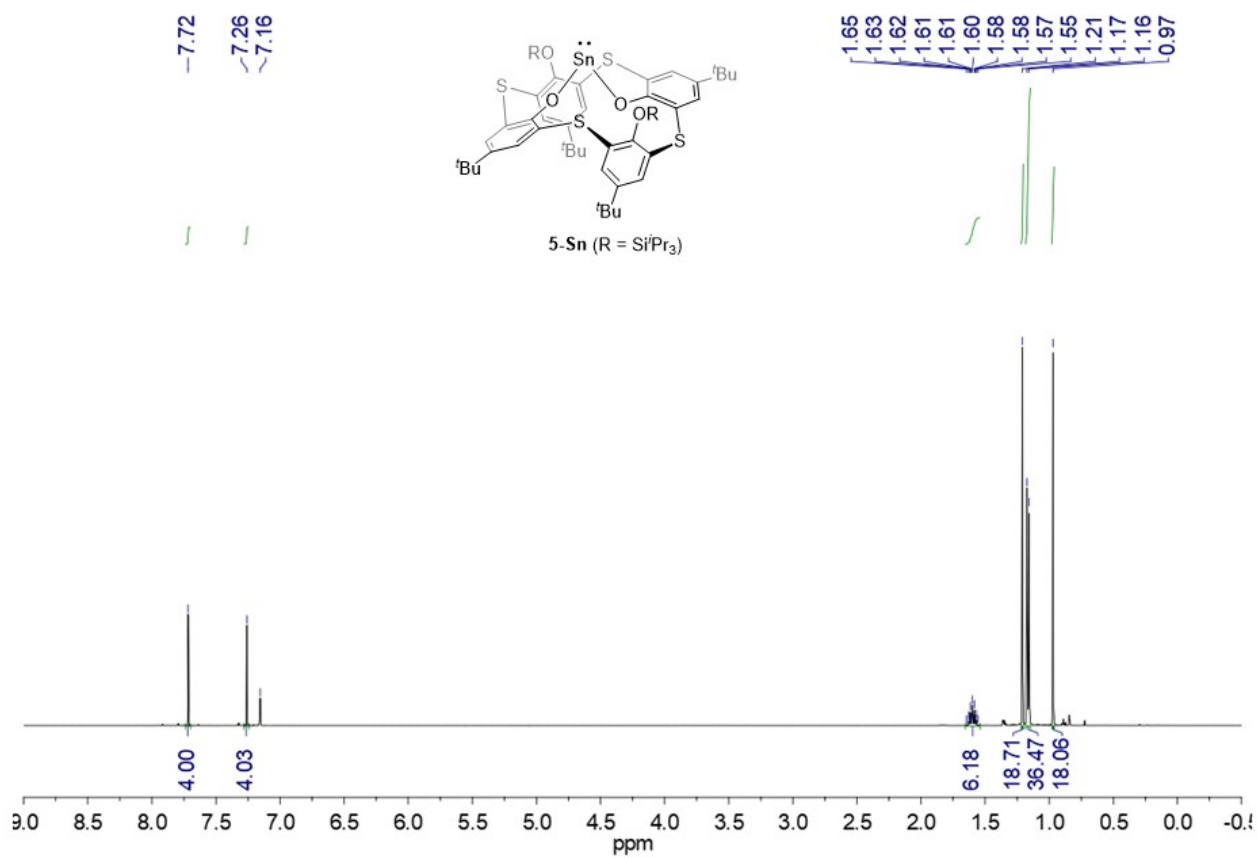


Figure S11. ^1H NMR spectrum of **5-Sn**.

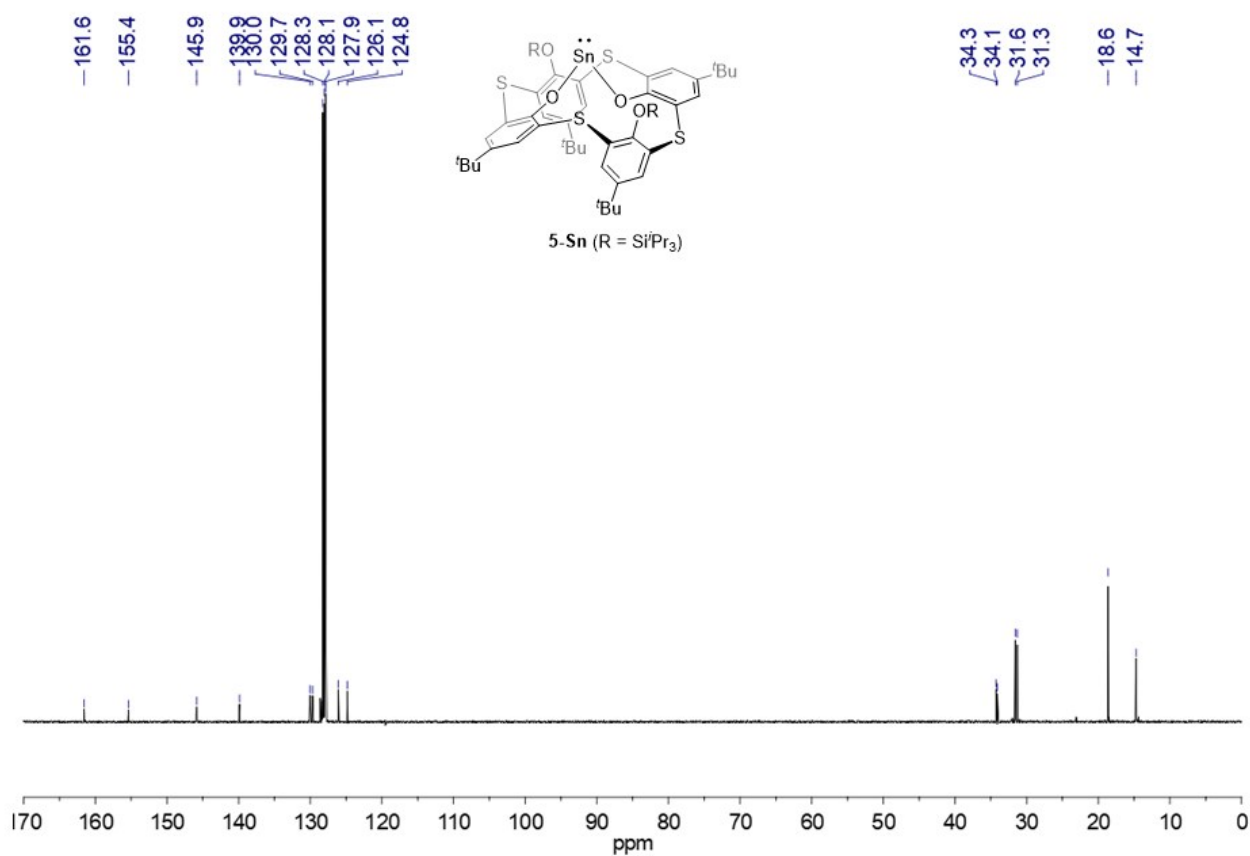


Figure S12. $^{13}\text{C}\{^1\text{H}\}$ NMR spectrum of **5-Sn**.

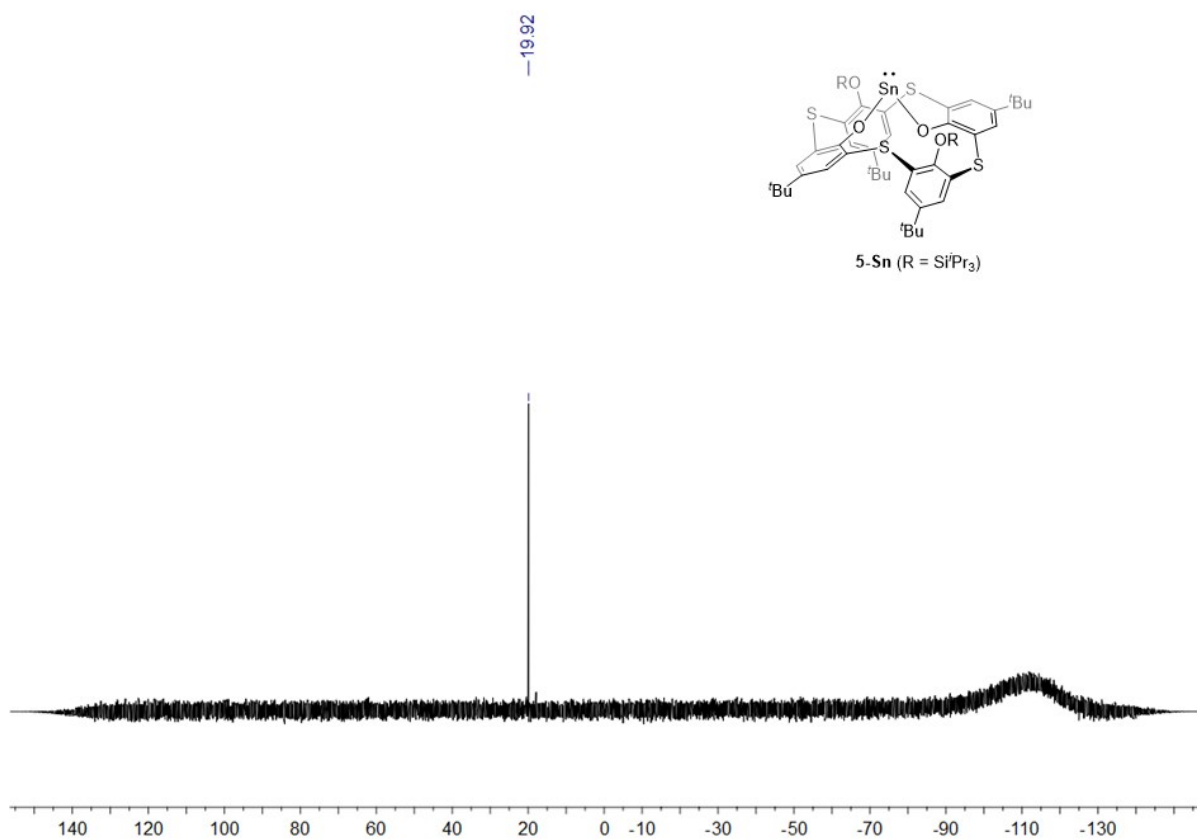


Figure S13. $^{29}\text{Si}\{^1\text{H}\}$ NMR spectrum of **5-Sn**.

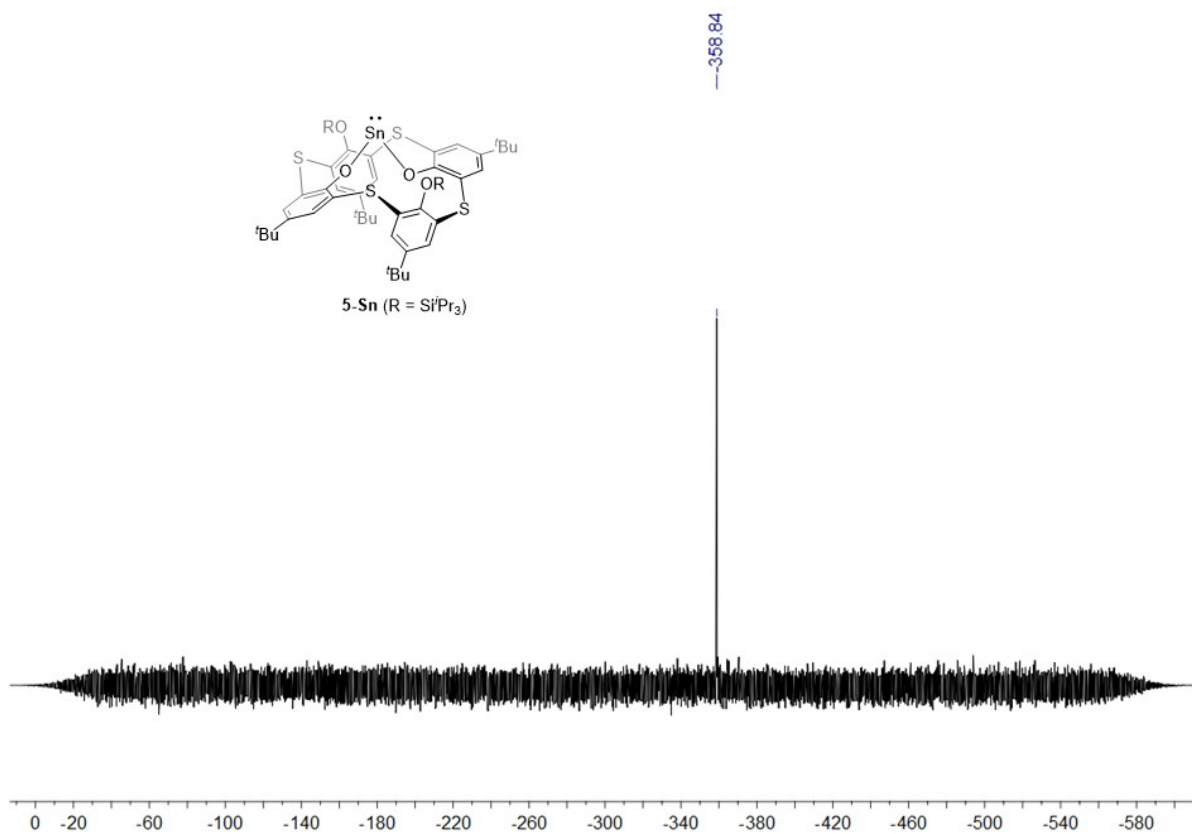


Figure S14. $^{119}\text{Sn}\{^1\text{H}\}$ NMR spectrum of **5-Sn**.

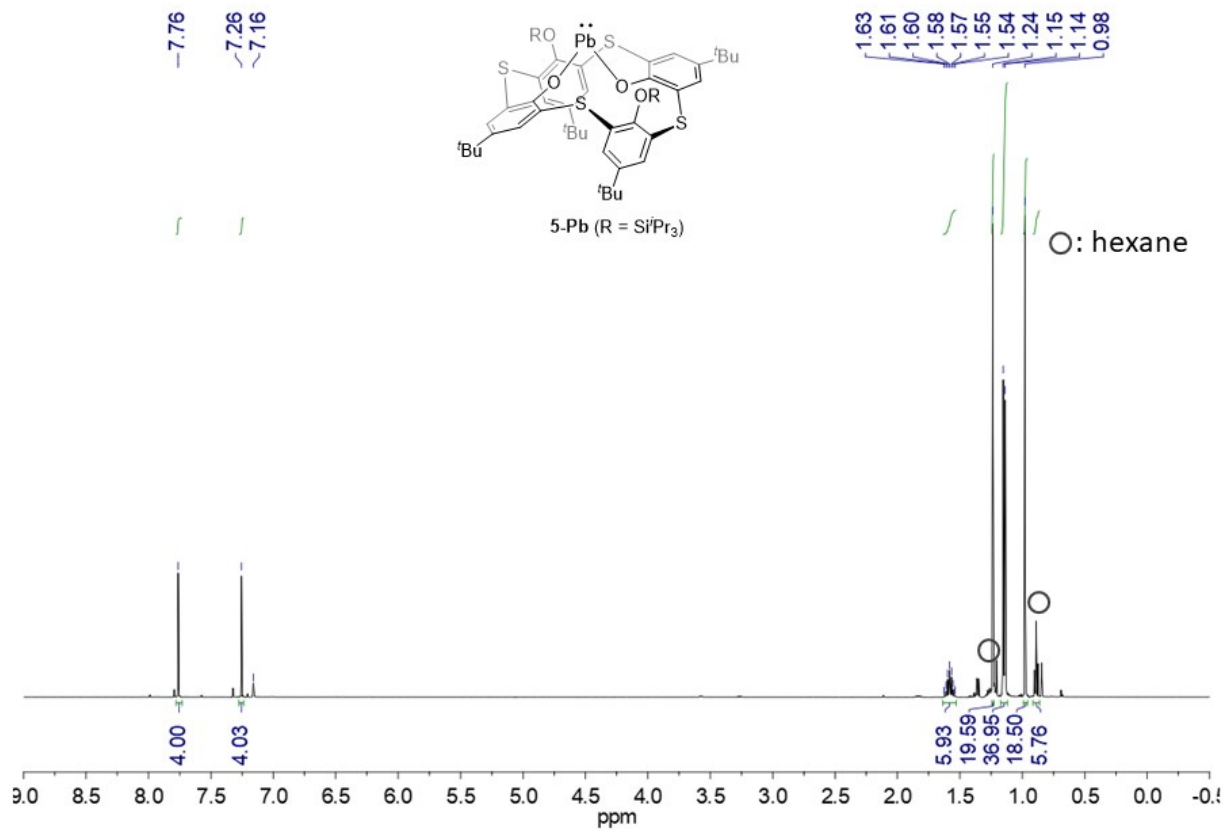


Figure S15. ^1H NMR spectrum of **5-Pb**.

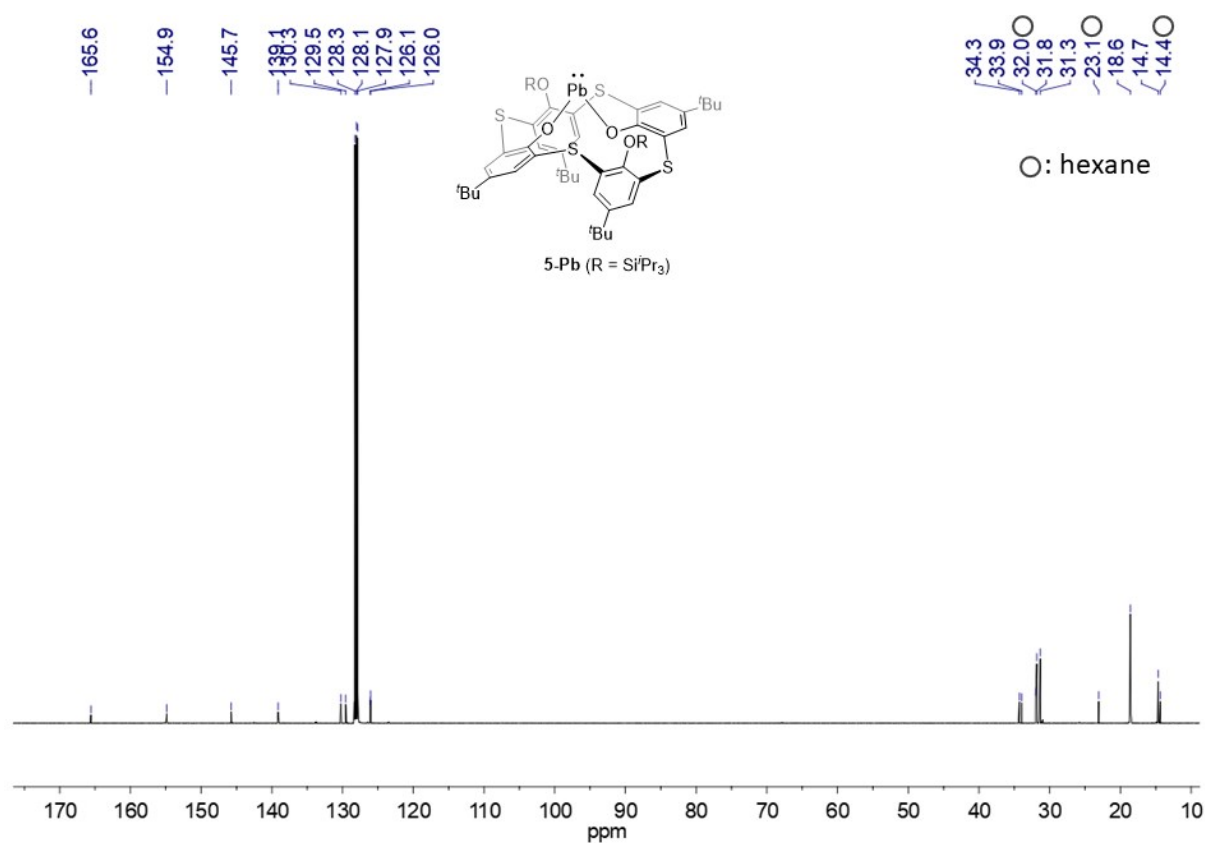


Figure S16. $^{13}\text{C}\{^1\text{H}\}$ NMR spectrum of **5-Pb**.

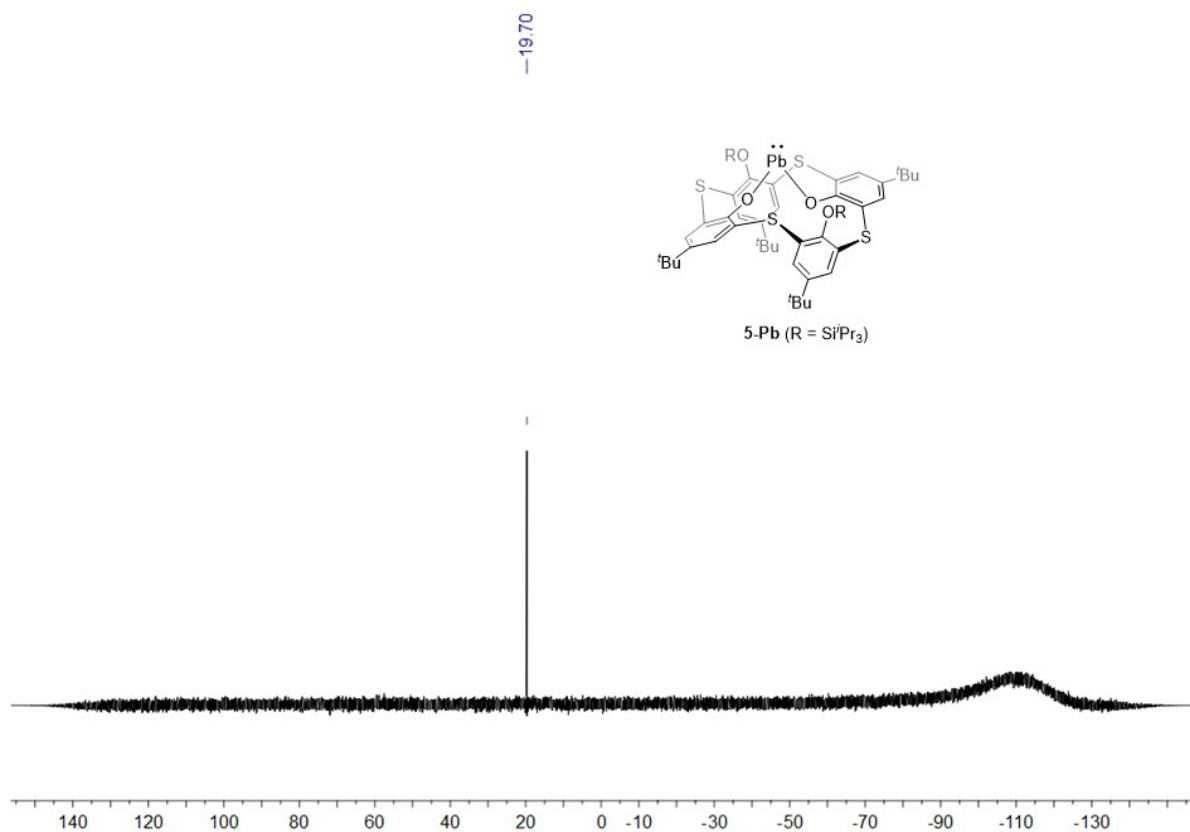


Figure S17. $^{29}\text{Si}\{^1\text{H}\}$ NMR spectrum of **5-Pb**.

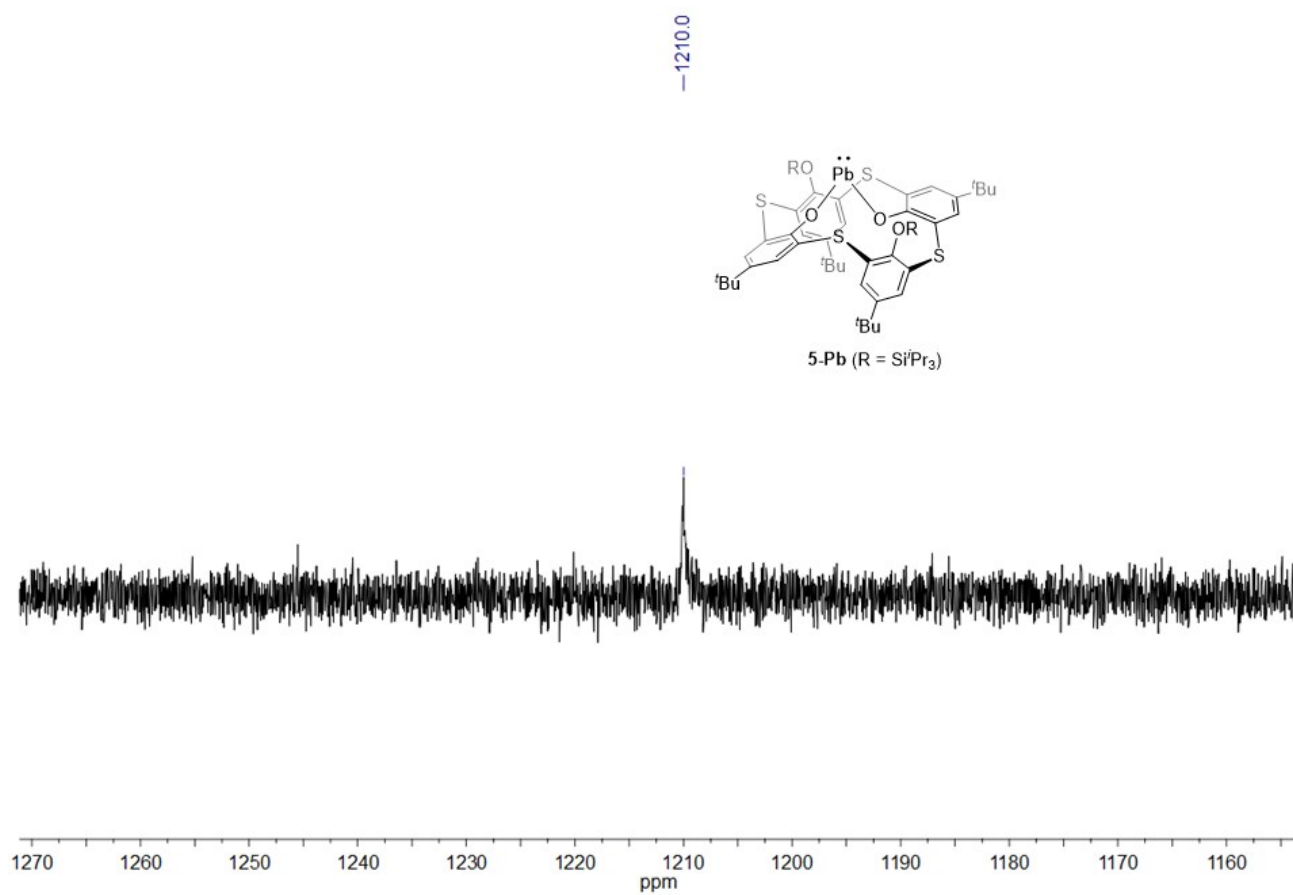


Figure S18. ^{207}Pb NMR spectrum of **5-Pb**.

5. References

- (1) Jacobson, R. A., *Private Communication to Rigaku Corp.; Rigaku Corp.; Tokyo Japan* **1998**.
- (2) *Crystal Structure 4.0: Single Crystal Structure Analysis Package; Rigaku Corp.; Tokyo, Japan* **2000-2010**.
- (3) Sheldrick, G., Crystal structure refinement with SHELXL. *Acta Crystallogr. Sec. C* **2015**, 71, 3-8.